International Research Journal of Advanced Engineering and Science
ISSN (Online): 2455-9024

Understanding the Controls on Clay Minerals Distribution in Modern Estuarine Sediments Through Integrated Geochemical and Petrographic Analysis

Dahiru Danjuma Muhammed[1]
[1]Department of Geology, University of Maiduguri, Nigeria.

Abstract— *Sandstone reservoirs in marginal marine catchments showed higher tendency of forming chlorite coated sand grains. In deeply buried sandstone reservoirs, these chlorite coats can enhance reservoir quality by inhibiting quartz overgrowth. However, limited understanding of the factors controlling clay mineral distribution makes it difficult to predict the occurrence of chlorite grain coats. This study examines Holocene sediment mineralogy and sub depositional environments within the estuarine catchment in West Cumbria NW England. A geochemistry-based classification scheme was used to identify palaeo sub depositional environments from core samples, and SEM EDS, grain size analysis, and image analysis were applied to investigate the distribution of clay minerals and clay coats. The sediments within the estuary catchment are dominated by quartz, K feldspar, plagioclase, muscovite, biotite, illite, chlorite, kaolinite, and smectite. Clay mineral distributions vary with sub environments: chlorite concentration is highest in the sand flat and tidal inlet and is present in a form of grain coat or as lithic grains in coarser sediment; kaolinite is most abundant in the mixed flat; smectite highest in the ebb tidal delta, north foreshore, and tidal inlet; illite is abundant in the salt marsh and mud flat. Clay occurs as pore filling or grain coating material in the salt marsh and mud flat settings, where coat coverage exceeds 40%. In the mixed flat, sand flat, and tidal bar, clay occurs mainly as grain coats, with coverage up to 40%. The tidal inlet, foreshore, and ebb tidal delta exhibit coat coverage of up to 5%. Overall, clay coat coverage increases with increasing clay fraction abundance. Sand flat and tidal bar sediments contain more than 10% detrital coat coverage and chlorite rich lithic grains, this is sufficient for the development of diagenetic chlorite coats capable of maintaining high porosity in deeply buried hydrocarbon reservoirs. The distribution of sediment mineralogy in the study area is controlled by grain size and estuarine hydrodynamics, while post depositional processes particularly early diagenetic alteration have modified clay mineral patterns in coarser sediments through feldspar alteration*

Keywords— *Resrvoir quality, clay coat, depostional environment, control, marginal marine.*

I. Introduction

Sandstone reservoirs deposited in marginal marine settings such as estuaries and deltas commonly develop clay coated sand grains (Pittman et al., 1992; Worden and Morad, 2003; Dowey et al., 2012; Dowey et al., 2017). Chlorite grain coats are particularly important because, in deeply buried reservoirs (>3000 m), they can inhibit quartz overgrowth and thereby preserve reservoir quality (Ehrenberg, 1993; Bloch and Helmold, 1995; Bloch et al., 2002; Worden and Morad, 2003; Ajdukiewicz and Lander, 2010; Ajdukiewicz and Larese, 2012; Worden et al., 2020). Consequently, sediment mineralogy and the extent of clay coat coverage exert a major control on porosity preservation in such sandstones. However, limited understanding of how depositional environments and post depositional processes influence the origin and distribution of these reservoirs enhancing clay minerals presents a challenge for predicting occurrence of clay coats in sandstone reservoirs.

The composition of sandstone reservoir is marginal marine is heterogeneous particularly clay distribution, as such numerous studies in these settings have linked sediment mineralogy particularly clay minerals to specific depositional environments (Dalrymple et al., 1992; Dowey et al., 2017; Wooldridge et al., 2017a; Wooldridge et al., 2017b; Griffiths et al., 2018; Griffiths et al., 2019a; Griffiths et al., 2019b; Wooldridge et al., 2019a). Clay minerals in such settings originate from three main pathways: inherited clays (Bokuniewicz, 1995; Aagaard et al., 2000; Tucker, 2001; Worden and Morad, 2003; Sionneau et al., 2008; Daneshvar and Worden, 2017; Zhang et al., 1990; Fan et al., 2008), neo formed clays (Bjørlykke, 1998; Worden and Morad, 2003), and transformed clays (Storvoll et al., 2002; Worden and Morad, 2003; Beaufort et al., 2015; Haile et al., 2015). Furthermore, clay mineral distribution in modern systems is also influenced by weathering patterns (Thiry, 2000; Tucker, 2001). Estuarine mineral distributions reflect the combined influence of marine and fluvial processes (Berner and Berner, 2012). Estuaries act as sediment traps during marine transgression (Boyle et al., 1974; Boyle et al., 1977; Dalrymple et al., 1992), and in situ mineral formation or alteration can occur shortly after deposition through neoformation or transformation processes (Berner, 1980; Aller and Aller, 1998; Feininger, 2013; McIlroy et al., 2003; Worden and Burley, 2003; Worden and Morad, 2003). Climatic conditions strongly influence clay types: mechanical weathering in cold climates favours chlorite and illite, whereas warm, humid conditions produce kaolinite, and semi-arid climates favour smectite formation (Eberl et al., 1984; Chamley, 1989; Rateev et al., 2008; Windom, 1976; Salem et al., 2000).Within estuaries, hydrodynamic forces—river flow, wave energy, and tides—redistribute sediment into specific sub environments such as salt marshes, mud flats, tidal bars, tidal inlets, foreshores, and ebb tidal deltas (Dalrymple et al., 1992). Sediment mineralogy can be affected by burial diagenesis through physicochemical processes (Grim and Johns, 1954; Griffin and Ingram, 1955; Powers, 1957; Nelson, 1960; Daneshvar and Worden, 2017) and biological activity (McIlroy et al., 2003; Needham et al., 2004; Worden et al., 2006). Examples include rapid clay alteration and biogenic silica accumulation in the Amazon Delta (Michalopoulos and

Dahiru Danjuma Muhammed, "Understanding the Controls on Clay Minerals Distribution in Modern Estuarine Sediments Through Integrated Geochemical and Petrographic Analysis," *International Research Journal of Advanced Engineering and Science*, Volume 11, Issue 1, pp. 145-156, 2026.

Aller, 1995; Aller and Michalopoulos, 1999; Michalopoulos et al., 2000; Michalopoulos and Aller, 2004). Diagenetic transformations relevant to estuarine settings include illite/kaolinite formation from feldspar alteration, chlorite transformation, and gibbsite precipitation (Drever and Zobrist, 1992; Huang, 1993; Velde and Church, 1999; Worden and Morad, 2003; Daneshvar and Worden, 2017). Understanding the primary depositional conditions is equally important on the distribution of clays, clay coats, and clay precursors (Ehrenberg, 1993; Saïag et al., 2016). Although detrital clays can form grain coats in tidal flat settings (Dowey et al., 2017; Wooldridge et al., 2017b; Wooldridge et al., 2019a), the full controls on their formation and distribution in marginal marine sands remain insufficiently understood (Worden and Morad, 2003; Dowey et al., 2017; Wooldridge et al., 2017b; Griffiths et al., 2018; Wooldridge et al., 2019a).

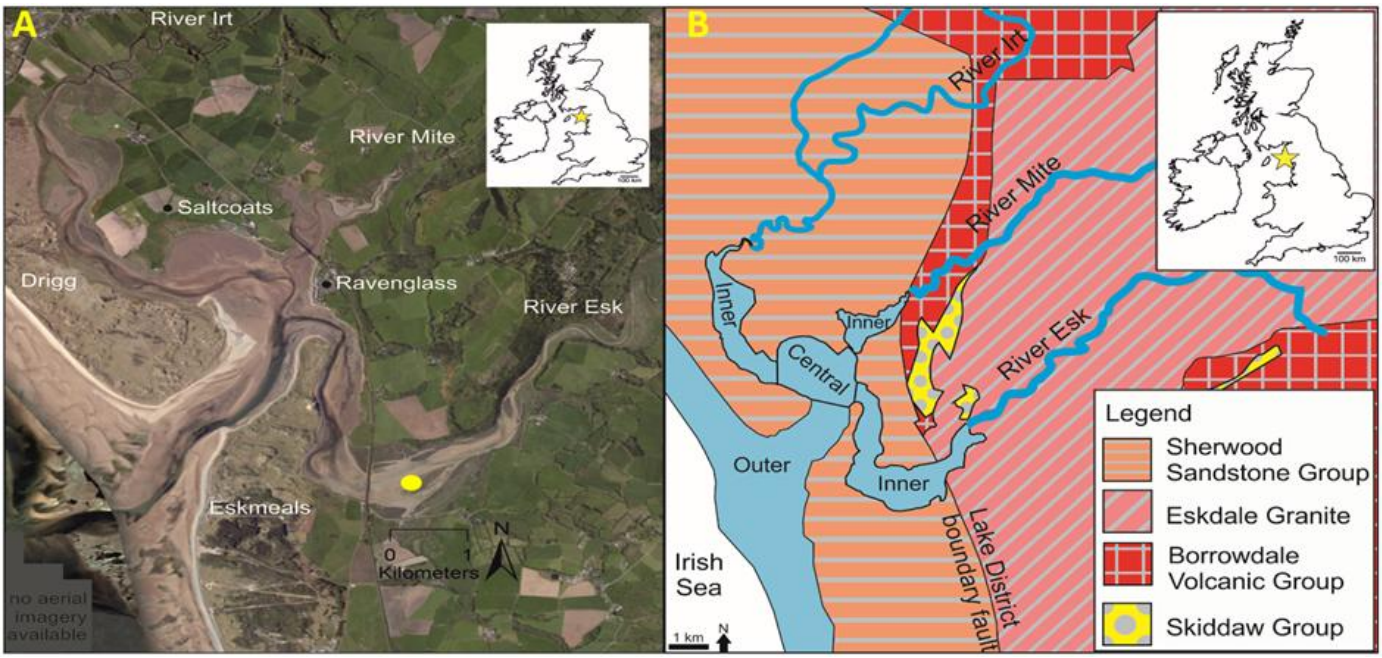

Figure 1. (A) Location map of the Ravenglass Estuary, north-west England with am inset map showing the location of the estuary in the UK, the yellow dot shows the location of geotechnical core. (B) Bedrock Geology of West Cumbria (Griffiths et al., 2018)

Hydrodynamic processes typically sort clay-sized and sand-sized particles (Virolle et al., 2019), this is why the mechanisms that incorporate clay minerals into sandy substrates remain poorly understood; previous studies have attributed this to clay infiltration and the effects of bioturbation (Matlack et al., 1989; Wilson, 1992; Worden and Morad, 2003; Needham et al., 2004; Needham et al., 2005; Needham et al., 2006; Worden et al., 2006; Saïag et al., 2016). Also, the origin and distribution of clay coats within sandstone reservoirs are poorly understood, fewer research work have examined modern clastic depositional systems such as tidal bars, making the prediction of clay-coat occurrence in reservoir-quality assessments particularly challenging (Ehrenberg, 1993; Worden and Morad, 2003; Wooldridge et al., 2017b). Although there are recent report on the origin and distribution of clay minerals and clay coats within the depositional environments of Ravenglass Estuary in NW Cumbria (Daneshvar, 2015; Daneshvar and Worden, 2017; Wooldridge et al., 2017a; Wooldridge et al., 2017b; Griffiths et al., 2018; Griffiths et al., 2019a; Griffiths et al., 2019b; Wooldridge et al., 2019a; Worden et al., 2020). The present study aims to advance understanding of sediment mineralogy and Holocene palaeoenvironments in an estuarine system, and to evaluate the relationships among clay abundance, clay-coat development, mineral alteration, and early diagenetic processes. The objectives of this research work are to are:

1. determine the mineral assemblage within the sub-depositional environment,
2. Determine minerals distribution and control,
3. Determine the predictability of mineral distribution as a function of sub-depositional environments.

Study area: West Cumbria Estuary

The study area in located in West Cumbria, it is a 5.6 km² macro tidal estuarine system located on the northwest coast of England, the estuary has a maximum tidal range of 7.55 m, exposing up to 86% of its area at low tide (Bousher, 1999; Lloyd et al., 2013; Wooldridge et al., 2017a; Wooldridge et al., 2017b; Griffiths et al., 2018; Griffiths et al., 2019a; Griffiths et al., 2019b). It extends landward to the tidal limits of the Rivers Mite, Irt, and Esk, and connects seaward to the Irish Sea through a 500 m wide tidal inlet bounded by the Drigg and Eskmeals coastal spits. These spits reduce wave action while allowing strong tidal currents due to the macro tidal regime. Sediment is supplied mainly by these three rivers, with average flow rates of 0.04 $m^3 s^{-1}$, 0.34 $m^3 s^{-1}$, and 0.42 $m^3 s^{-1}$, respectively (Bousher, 1999). The estuary is tide and wave dominated (Kelly et al., 1991), and its shallow bathymetry produces tidal asymmetry, characterised by a longer ebb flow than flood flow.

Dahiru Danjuma Muhammed, "Understanding the Controls on Clay Minerals Distribution in Modern Estuarine Sediments Through Integrated Geochemical and Petrographic Analysis," *International Research Journal of Advanced Engineering and Science*, Volume 11, Issue 1, pp. 145-156, 2026.

Salinity conditions vary spatially: the inner estuary is brackish, the central Saltcoats tidal flat area has mixed energy conditions with near marine salinity, and the outer estuary—comprising the main tidal channel, mouth, and foreshore—is fully marine with wave and tidal influence. Human impact is limited due to sparse settlement, though construction of a railway bridge in 1868 promoted salt marsh expansion and protected the lower River Mite from tidal energy (Carr and Blackley, 1986). Geology of the Study Area.

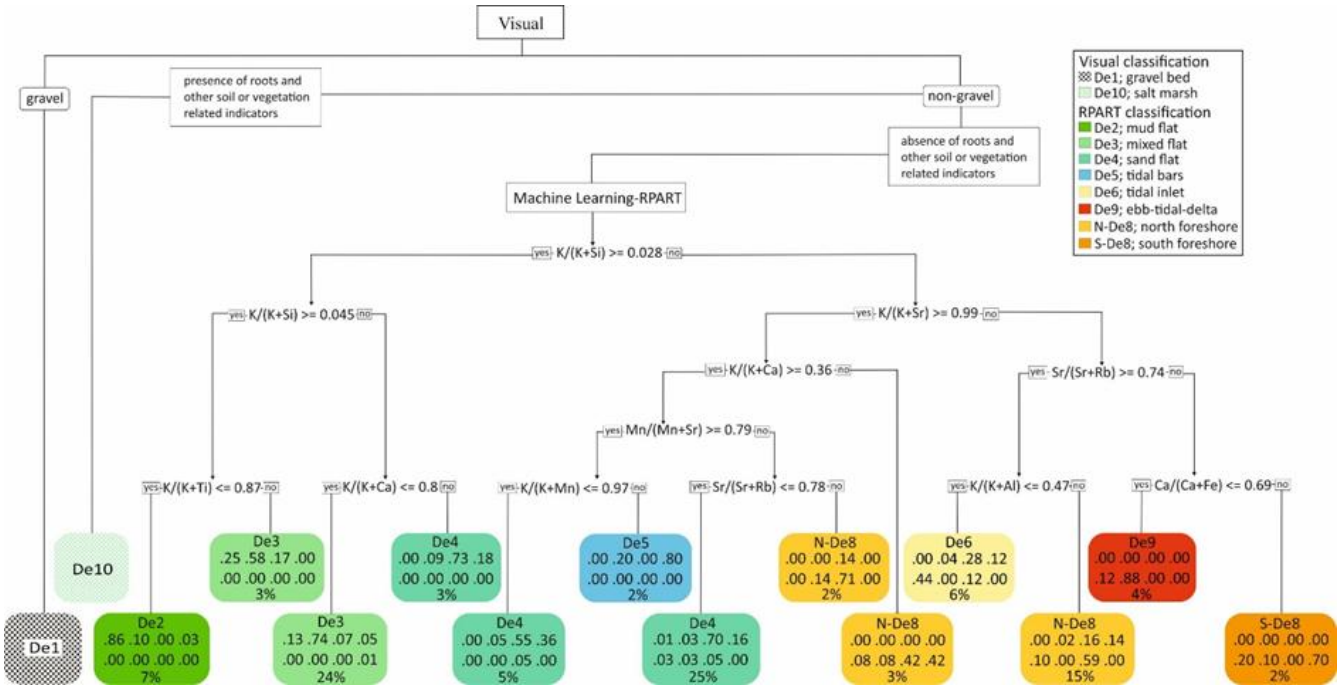

Figure 2. Classification tree for the discrimination of estuarine paleo-sub-depositional environments, developed through a combination of visual analysis and multi-element XRF analyses, using supervised classification and the recursive partitioning package, RPART (Therneau and Atkinson, 2019; R Core Team, 2016). This RPART supervised machine learning approach differentiated De2, De3, De4, De5, De6, NDe8, SDe8 and De9 based on multi-element analyses of K/(K+Si), K/(K+Al), K/(K+Ca), K/(K+Ti), K/(K+Mn), K/(K+Sr), Sr/(Sr+Rb), Ca/(Ca+Fe), and Mn/(Mn+Sr) indices data. In each leaf node, the fraction of samples in that specific classification category are listed as fractional quantity and where these fractional values are less than 1.00, the uncertainty is as a result of some depositional environments having an overlapping attribute, even when nine dimensions are considered. This classification tree has a model accuracy of 72.3 % (Muhammed et al., 2022).

Sediments in West Cumbria Estuary catchment are sourced from a range of different bedrock types and Quaternary drift-deposits (Daneshvar and Worden, 2017; Griffiths et al., 2018; Griffiths et al., 2019a; Griffiths et al., 2019b). The source area is composed of the Devonian Eskdale Granite, the Ordovician Borrowdale Volcanic Group (BVG), the Triassic Sherwood Sandstone Group and the Cambrian Skiddaw Group slate. The Devonian Eskdale Granite is the largest exposed intrusion in Cumbria (Soper, 1987) and forms part of the Lake District Batholith along the western margin of the massif (Quirke et al., 2015). Hydrothermal alteration of its mafic silicates and plagioclase has produced significant chlorite alteration (Moseley, 1978; Rundle, 1979; Young et al., 1986; Quirke et al., 2015). The Skiddaw Group consists of fine grained metapelitic sedimentary rocks that have undergone weak metamorphism (Merritt and Auton, 2000). The Ordovician Borrowdale Volcanic Group (BVG) occurs in two outcrops an older northwestern and a younger south eastern unit (Entwisle et al., 2005). This subduction related volcanic rocks include K rich calc alkaline basalt to rhyolite, sills, and pyroclastics, forming the central Lake District massif (Millward, 2004; Quirke et al., 2015). During the Caledonian Orogeny (~395 Ma), they experienced sub greenschist metamorphism and multiple hydrothermal events producing complex alteration zones and vein haematite (Milodowski et al., 1998; Entwisle et al., 2005). To the west, a small area of the Triassic Sherwood Sandstone Group (St Bees Sandstone Formation) forms a feldspathic, fluviatile sandstone sequence (Strong et al., 1994) dominated by detrital quartz, subordinate feldspar, muscovite, biotite, albite, and carbonate clasts (Barnes et al., 1994; Strong et al., 1994), along with heavy minerals such as zircon, tourmaline, apatite, anatase and rutile (Strong et al., 1994). The Quaternary drift deposits within the study area comprise glacial till, peat, and glaciolacustrine sediments (Merritt and Auton, 2000; Griffiths et al., 2018; Griffiths et al., 2019a; Griffiths et al., 2019b). The Holocene succession records nearly 10,000 years of deposition (McGhee et al., 2021). Glacial till knolls are exposed across the estuary, with peat commonly overlying the glacial deposits (Lloyd et al., 2013).

II. Samples and Methods

Core Data

Sediment cores were collected through the Holocene succession within the vegetated tidal-bar sub-depositional environment of the inner estuary, located in the Esk arm of the Estuary (Fig. 1A). Drilling was undertaken by Geotechnical

Engineering Ltd (GEL) as reported in McGhee et al. (2021). Three cores were obtained, measuring 5 m, 7 m, and 10 m in length for BH07, BH08, and BH10 respectively. All cores were drilled using a lightweight Geotechnical Engineering Ltd "Pioneer" rotary rig, selected specifically due to the soft and unconsolidated nature of the sediment surface.

The recovered cores were housed in 12 cm-diameter, 1 m-long semi-rigid plastic liners to ensure protection and allow easy transport. Each 1 m core section was split, photographed when it is wet and dry. Detailed sedimentary logging was conducted, the logs were produced at a scale of 1:5, with lithofacies characterised based on grain-size distribution, colour, sedimentary structures, bed thickness, presence of roots and shell fragments, and the intensity and type of bioturbation. Subsampling at 5cm interval was carried out throughout all core sections. These samples were analysed for XRF and LPSA.

XRF analysis

X ray fluorescence (XRF) analysis was carried out using a portable Thermo Scientific Niton XL3t GOLDD spectrometer to quantify the concentrations of major and trace geochemical elements. The portable XRF instrument is a fully integrated, energy dispersive system equipped with a variable intensity X ray source (6–50 kV, 0–200 µA Ag anode tube) and a factory calibrated GOLDD (Geometrically Optimised Large Area Drift Detector) system. This configuration enables low detection limits and high precision measurement of more than 40 elements. Instrument accuracy and precision were evaluated by analysing a single sample 30 times. The resulting mean concentrations (ppm), with standard deviations in parentheses, were as follows: Al – 64,099 (1,685), Si – 376,925 (4,191), K – 18,234 (145), Ca – 2,610 (46), Ti – 2,477 (92), Fe – 11,837 (90), Mn – 172 (19), Rb – 70 (1), Sr – 73 (2), Zr – 352 (3), Ba – 487 (18), and Cs – 85 (4). Each measurement was performed for 150 seconds in "Test All GEO" mode. This duration was selected after iterative testing in which repeated analyses were conducted under progressively longer measurement times until further reductions in analytical uncertainty were no longer observed.

TABLE 1. Mineralogical composition Holocene core sediment from SEM-EDS analysis

Depth cm	Depositional environments	Coat coverage	Mean grain size	Clay fraction	Quartz	Plagioclase	K-Feldspar	Muscovite	Biotite	Carbonates	Chlorite	Kaolinite	Smectite	Illite
64	Saltmarsh	58	29	0.0548	44	6	6	2.68	1.95	4.53	1.45	5.86	0.66	20.26
115	Mixed flat	41	140	0.0161	79	4	5	0.72	0.61	0.51	0.79	1.11	0.24	3.82
154	Sand flat	10	114	0.0174	75	8	8	0.33	0.45	0.04	1.39	0.42	0.21	1.54
206	Sand flat	33	180	0.0105	82	6	3	1.02	0.27	0.52	0.89	0.81	0.10	2.24
251	Sand flat	7	170	0.0115	60	16	7	2.82	2.13	0.01	5.13	0.46	0.68	3.27
306	Sand flat	7	230	0.0075	82	4	6	1.07	0.51	0.53	0.68	0.87	0.15	1.34
63	Saltmarsh	46	114	0.0204	68	6	8	0.87	1.03	2.51	0.97	1.68	0.13	6.80
86	Saltmarsh	41	103	0.0333	56	6	5	1.62	2.48	3.69	1.11	2.26	0.40	16.69
300	Mixed flat	5	420	0.0027	70	12	6	2.84	1.24	0.67	1.17	0.87	0.36	2.83
110	Sand flat	9	188	0.0065	83	5	6	0.63	0.94	0.43	1.06	0.15	0.12	1.21
135	Sand flat	29	190	0.0063	80	3	8	1.91	0.72	0.37	0.84	0.43	0.23	1.91
183	Sand flat	16	198	0.0089	82	5	6	0.59	0.35	1.02	0.50	0.46	0.13	1.20
230	Sand flat	5	269	0.0028	77	7	4	2.23	0.53	0.02	2.46	1.03	0.28	2.14
270	Sand flat	8	281	0.0038	75	6	12	0.71	0.44	0.31	1.51	0.65	0.15	1.10
390	Tidal inlet	3	474	0.0030	80	5	7	1.02	0.49	1.37	0.73	0.23	0.18	1.40
335	North foreshore	6	413	0.0025	71	12	5	0.70	2.19	1.61	1.85	0.14	0.34	2.79
360	North foreshore	5	491	0.0026	80	7	5	0.44	1.05	0.88	0.86	0.48	0.40	1.63
450	North foreshore	3	296	0.0041	76	8	9	0.81	1.07	0.19	0.94	0.24	0.30	1.91
480	North foreshore	7	296	0.0044	83	4	6	0.46	0.58	1.08	0.72	0.36	0.19	0.93
560	North foreshore	5	314	0.0042	80	6	6	0.99	0.79	1.64	0.45	0.45	0.18	1.47
33	Saltmarsh	44	16	0.0776	36	7	3	3.30	2.84	1.84	2.16	6.29	0.72	28.59
73	Saltmarsh	61	12	0.0964	27	8	3	3.25	4.26	1.95	2.29	6.09	0.69	32.32
118	Saltmarsh	45	24	0.0577	49	8	5	2.25	1.42	4.06	1.66	3.89	0.53	14.81
143	Saltmarsh	39	32	0.0422	61	10	6	1.72	1.14	3.36	1.48	1.82	0.45	8.04
173	Saltmarsh	47	25	0.0492	28	6	3	3.82	5.60	2.39	2.09	9.06	0.46	29.54
193	Mud flat	43	27	0.0406	55	9	6	2.11	1.58	2.19	1.87	1.95	0.46	14.87
223	Mixed flat	19	75	0.0204	70	7	8	1.23	0.71	3.61	0.42	1.86	0.17	2.64
273	Sand flat	5	440	0.0016	55	13	4	2.48	1.53	0.00	13.96	1.59	0.99	3.51
293	Sand flat	3	330	0.0027	80	6	6	0.63	0.96	0.02	1.46	0.91	0.28	1.30
450	Sand flat	6	333	0.0043	82	6	5	0.63	0.86	0.02	0.73	0.64	0.08	1.68
787	Sand flat	8	334	0.0040	84	5	2	0.76	0.43	0.01	1.27	0.95	0.26	1.73
383	Ebb-tidal-delta	3	530	0.0017	85	6	3	0.99	0.52	0.01	0.57	0.51	0.25	1.61
640	North foreshore	6	297	0.0059	80	5	5	1.15	0.76	0.03	1.24	1.23	0.34	1.68
680	North foreshore	10	288	0.0071	71	12	8	1.10	0.68	0.02	0.78	1.05	0.31	1.75
742	North foreshore	6	345	0.0050	74	9	5	1.09	1.76	0.02	1.36	0.70	0.43	3.53

Dahiru Danjuma Muhammed, "Understanding the Controls on Clay Minerals Distribution in Modern Estuarine Sediments Through Integrated Geochemical and Petrographic Analysis," *International Research Journal of Advanced Engineering and Science*, Volume 11, Issue 1, pp. 145-156, 2026.

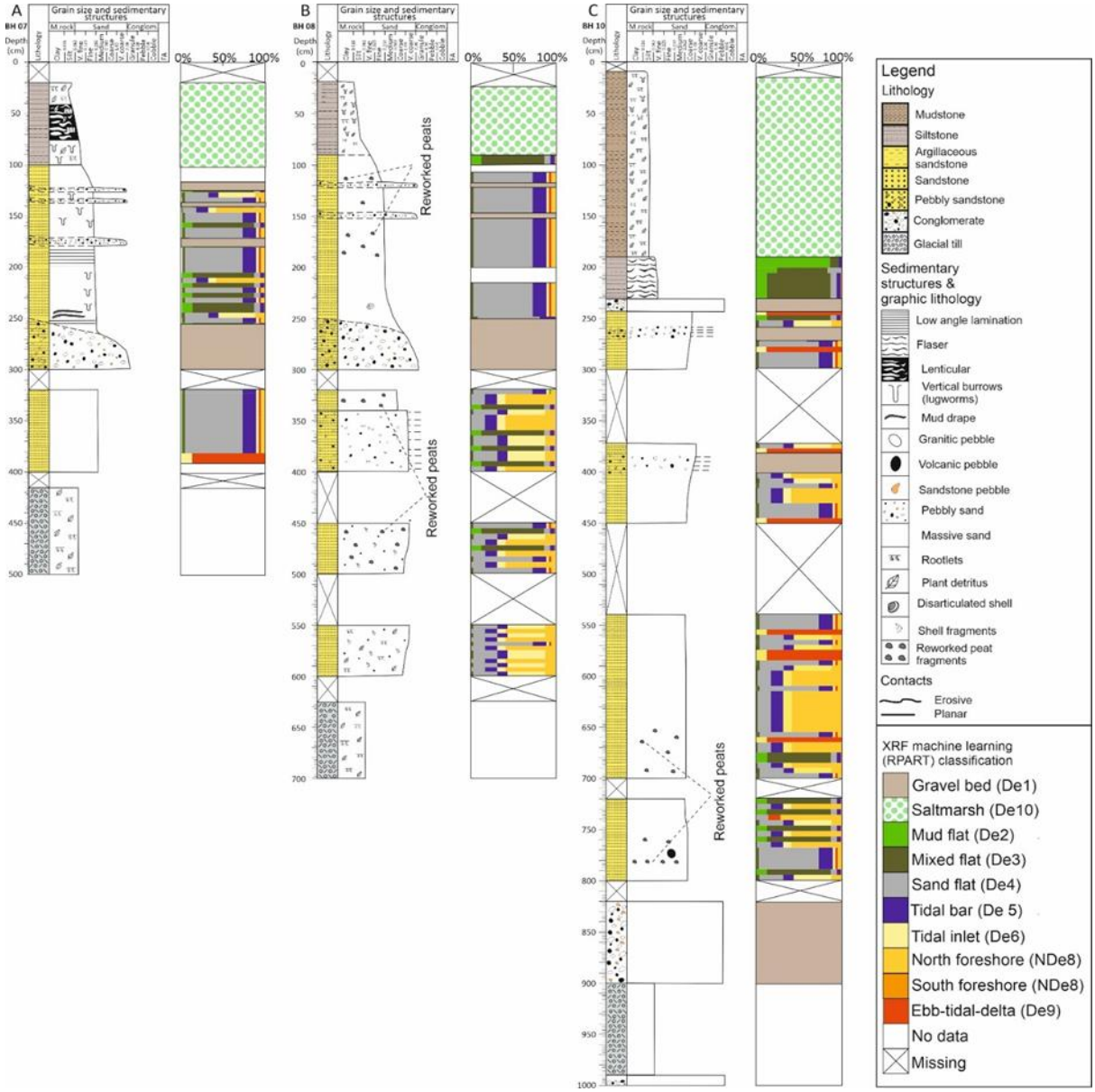

Figure 3. Figure Schematic sedimentary log of inner estuary vegetated tidal bars deposits with application of the classification tree in Figure 2. Showing the graphic log of a core from a tidal bar in the inner estuary with the interpreted sub-depositional environments presented in the column to the right of the graphic log following application of the classification diagram.

Interpretation of palaeo-sub-depositional environment

A classification tree (Fig. 2) was developed to discriminate the sub-depositional environments from the core samples, using a combination of visual assessment and multi-element XRF data, employing supervised classification approach in RPART package (Therneau and Atkinson, 2019; Muhammed et al., 2022). The approach begins with visually identifying gravel beds (De1) and vegetated salt marsh (De10) based on the presence of pebbles, roots, and plant detritus. Subsequent classification uses the RPART model, where each decision node splits data according to a single geochemical variable. Leaf nodes list the predicted depositional environment, accompanied by the fractional proportion of samples supporting that classification, which reflects the certainty of the decision. The percentage of total samples contained within each leaf node is also shown. This method differentiates De2, De3, De4, De5, De6, NDe8, SDe8, and De9 using pXRF-derived ratios including K/(K+Si), K/(K+Al), K/(K+Ca), K/(K+Ti), K/(K+Mn), K/(K+Sr), Sr/(Sr+Rb), Ca/(Ca+Fe), and Mn/(Mn+Sr)

Grain size analysis

Prior to grain-size measurement, organic matter was removed from the samples through chemical digestion, a necessary pre-treatment step because organic components can impede sediment dispersion and bias grain-size results. After digestion and then freeze drying, Calgon (sodium hexametaphosphate) was added for adequate sediment dispersion and homogenisation. This ensures that individual

Dahiru Danjuma Muhammed, "Understanding the Controls on Clay Minerals Distribution in Modern Estuarine Sediments Through Integrated Geochemical and Petrographic Analysis," *International Research Journal of Advanced Engineering and Science*, Volume 11, Issue 1, pp. 145-156, 2026.

particles are fully separated before laser analysis, an essential condition for obtaining accurate and reproducible particle-size distributions. The laser particle size analysis (LPSA) was conducted following the procedures outlined by Simon et al. (2021). Sediment samples were first sieved to exclusively collect the <2 mm sand fraction, the <2 mm sand fraction was then analysed using a Beckman Coulter laser particle size counter, an instrument capable of generating high-resolution particle-size distributions by measuring light scattering patterns as particles pass through a laser beam. The result from LPSA provide detailed information on the proportion of clay, silt, and sand-sized particles present. GRADISTAT© software package was used to processed and commute the LPSA output into meaningful statistical textural parameters such as mean grain size, sorting, skewness, and kurtosis.

Mineral Analysis

Sediment mineralogy was characterized using automated mineralogical analysis via SEM–EDS. This was performed with a FEI WellSite QEMSCAN® system, which integrates a scanning electron microscope with energy dispersive spectrometers to analyze mineral chemistry. The instrument operates using a 15 kV electron beam and two Bruker EDS detectors, enabling the measurement of primary and secondary backscatter electrons. In the images generated by the instrument, brightness reflects sample density, while surface signal variations indicate differences in atomic weight. The QEMSCAN system includes an electronic processing unit and the iDiscover software suite that utilises a Species Identification Protocol (SIP). This protocol uses a mineralogical chemical database stored in the system's library to identify and quantify mineral phases within the samples. Mineralogical determination is fully quantitative: each sample is subdivided into 2 mm × 2 mm analytical fields, and each field is analyzed individually. SEM–EDS analysis was done using a carbon coated polished thin sections, with data collected using a user defined step size of 2 µm to ensure that all clast sizes were adequately captured. The spatial resolution of the resulting datasets depends directly on the chosen step size. The final output is a detailed mineral map, providing both quantitative mineral abundances and accompanying textural information for each analyzed sample.

Clay-coat coverage

Clay coat coverage was quantified using the perimeter tool in Petrog software, developed by Wooldridge et al. (2019b). This tool measures clay coat coverage on SEM backscattered electron images by first defining the total grain perimeter and then identifying the portion covered by attached clay coat. A total of 2,160 SEM images, containing approximately 60 sand grains per sample, were analyzed. Only clay coating in direct and continuous contact with a grain was classified as a clay coat; diffuse clay webs or aggregates without continuous attachment were excluded.

III. Results And Discussions

Sediment mineralogy

The SEM–EDS analysis identified a diverse mineral assemblage within the cores. Quartz is the dominant with concentration ranging between 27.4–85.4%. Plagioclase and K feldspar each range from 2.1–15.7%. Carbonates, biotite, and muscovite are present in minor amounts (0.1–5.6%). The clay minerals, chlorite ranges from 0.4–14.0%, illite from 0.9–32.2%, kaolinite from 0.1–9.1%, and smectite from 0.1–1.0%.

Mineral Abundance

The relationships between mineral abundance, grain size, and clay fraction across the sub depositional environments are shown in Figure 4. Quartz is most concentrated in coarse sediments (>200 µm) from the ebb tidal delta, north foreshore, tidal inlet, sand flat, and mixed flat, and least abundant in the clay rich salt marsh and mud flat settings. K feldspar and plagioclase occur mainly in sediments with low clay content (<0.02%), with highest concentrations in the mixed flat, mud flat, and north foreshore; K feldspar is also elevated in the sand flat and tidal inlet, and both feldspars are least abundant in the ebb tidal delta. Biotite and muscovite increase with clay fraction above 0.02% and are most abundant in the mud flat and salt marsh, with muscovite also elevated in the mixed flat; both minerals are lowest in the ebb tidal delta, north foreshore, and tidal inlet. Chlorite remains uniformly low (<3%) but shows a slight increase where clay content exceeds 0.02%. Kaolinite is most abundant in fine grained sediment (<62 µm) and increases with clay content above 0.02%. Smectite varies across finer sediments but shows a minor increase in samples with grain sizes >200 µm and clay content above 0.02%. Illite is most abundant in fine grained settings but decreases slightly in sediments finer than 70 µm, then increases substantially when clay content exceeds 0.02%.

Clay Minerals Abundance

Figure 5 shows that the relative abundances of chlorite, illite, smectite, and kaolinite vary systematically across the sub depositional environments. Chlorite is most abundant in the sand flat and tidal inlet, moderate in the north foreshore and ebb tidal delta, and consistently low in the mud flat, mixed flat, and salt marsh. Kaolinite is slightly higher in the mixed flat and shows broadly similar, intermediate values across all other environments. Smectite is most abundant in the ebb tidal delta, north foreshore, and tidal inlet, moderate in the sand flat and mixed flat, and low in the mud flat and salt marsh. Illite is most abundant in the salt marsh and mud flat and shows similar intermediate values across the remaining environments.

Clay Coat Coverage

Clay coat coverage increases with clay fraction abundance. It is highest in the mud flat, mixed flat, and salt marsh environments, reaching up to 40%. Sand flat sediments show average coverage above 7%, while the tidal inlet, north foreshore, and ebb tidal delta display less than 5%. Overall, clay coat coverage varies markedly among the sub depositional environments.

Dahiru Danjuma Muhammed, "Understanding the Controls on Clay Minerals Distribution in Modern Estuarine Sediments Through Integrated Geochemical and Petrographic Analysis," *International Research Journal of Advanced Engineering and Science*, Volume 11, Issue 1, pp. 145-156, 2026.

International Research Journal of Advanced Engineering and Science
ISSN (Online): 2455-9024

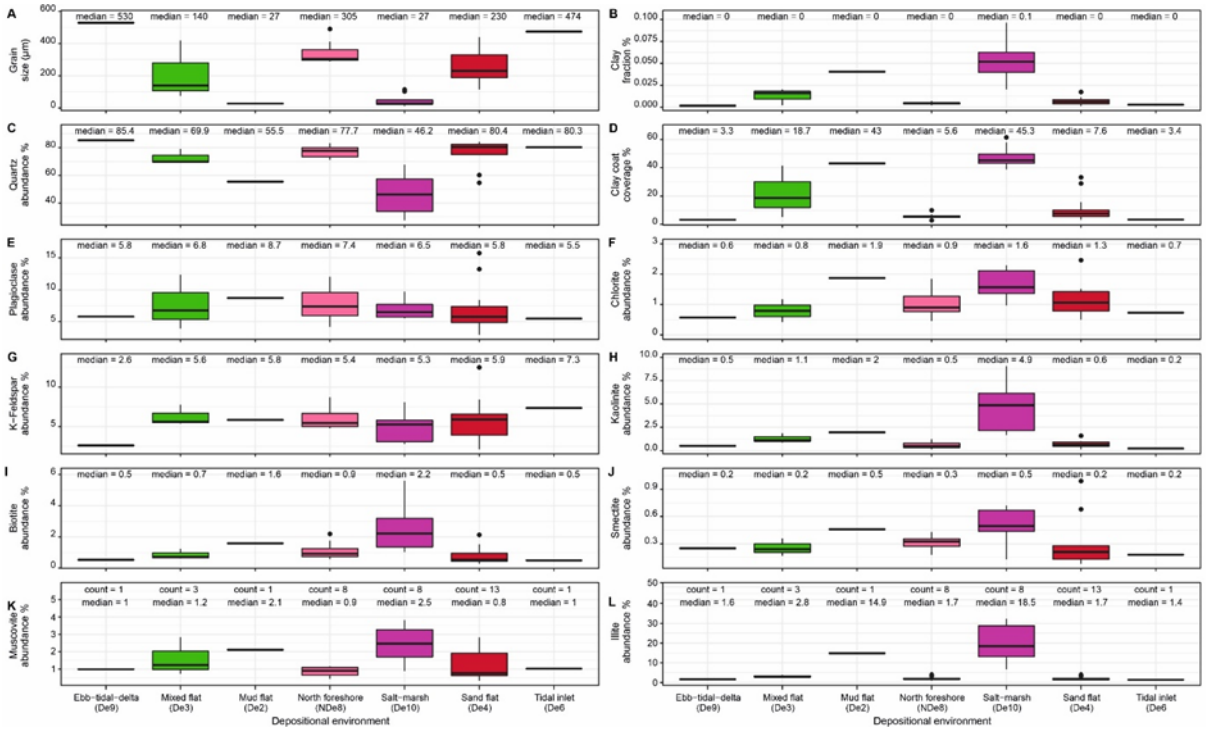

Figure 4. Box plots for sediment parameters as a function of West Cumbria Estuary interpreted paleo-sub-depositional environment of; (A) Grain size (mm), (B) clay fraction (C) quartz abundance, (D) clay coat coverage, (E) plagioclase abundance, (F) chlorite abundance, (G) k-feldspar abundance, (H) kaolinite abundance, (I) biotite abundance, (J) smectite abundance, (K) muscovite abundance, (L) illite abundance. Feldspar abundance does not depend on grain size but varies by sub depositional environment: plagioclase is most common in the mixed flat, mud flat, and north foreshore, while K feldspar is most abundant in the mixed flat, mud flat, sand flat, tidal inlet, and north foreshore. Micas are most abundant in fine grained sediments, with biotite concentrated in the mud flat and salt marsh, and muscovite in the mud flat, mixed flat, and salt marsh. Clay coat coverage increases with clay fraction abundance and is highest in the mud flat, mixed flat, and salt marsh. Chlorite distribution is relatively uniform and unrelated to clay fraction or coat coverage. Kaolinite is most abundant in the salt marsh and elevated in the mud and mixed flat. Smectite abundance mirrors clay coat patterns across several environments. Illite is most abundant in the mud flat and salt marsh and remains low elsewhere.

Figure 5. Clay mineral abundance as a function of estuarine sub-depositional environments (A) Chlorite index. (B) Kaolinite index. (C) Smectite index. (D) illite index.

Dahiru Danjuma Muhammed, "Understanding the Controls on Clay Minerals Distribution in Modern Estuarine Sediments Through Integrated Geochemical and Petrographic Analysis," *International Research Journal of Advanced Engineering and Science*, Volume 11, Issue 1, pp. 145-156, 2026.

Sediment Mineral Assemblages

The distribution of sediment mineralogy in clastic sediments is governed by several factors, including the geological characteristics of the source area, the intensity and extent of weathering, the vigour and transport distance of the fluvial system, and the redox conditions at the depositional site (Fralick and Kronberg, 1997). Post depositional modifications such as in situ weathering and mineral biological interactions including bioturbation, microbial processes, and soil forming mechanisms can further alter the mineralogical characteristics of clastic sediments (Daneshvar and Worden, 2017).

In the studied core samples, sediments are strongly dominated by quartz, with quartz representing approximately 69% of the total mineral assemblage (Table 1; Fig. 4). The estuarine sediment composition is classified as arkosic to subarkosic, reflecting derivation from the Eskdale Granite, Sherwood Sandstone, and andesitic units of the Borrowdale Volcanic Group in the hinterland (Daneshvar and Worden, 2017; Griffiths et al., 2019a). Feldspar distribution appears independent of grain size but varies with different sub depositional environments, whereas mica abundance is highest within finer grained sediments and shows marked variation across these environments.

The occurrence of iron bearing lithic fragments such as chlorite and biotite has been reported within both the Borrowdale Volcanic Group (Quirke et al., 2015) and the Eskdale Intrusions (Moseley, 1978; Young et al., 1986; Quirke et al., 2015). Consequently, the iron rich lithics observed in the study area (Fig. 6C) were likely sourced from these older rocks, and the chlorite present is interpreted as a detrital mineral. Carbonate occurrences within the sediments are likely derived primarily from shell rich gravel layers, given the absence of major carbonate bedrock within the source area.

Clay minerals distribution

The distribution of clay minerals across the paleo sub depositional environments the study area is shown in Figure 5. Illite is the most abundant clay mineral, while chlorite and kaolinite occur in lower proportions, and smectite is the least abundant. This pattern aligns with global oceanic clay mineral trends (Rateev et al., 2008). The high relative abundance of illite and kaolinite within the mud dominated sub depositional environments indicates that these minerals predominantly occur in the clay grade fraction (Fig. 5B, 5D). In contrast, the elevated proportions of chlorite and smectite in sand dominated environments combined with their presence within lithic grains observed in SEM imaging suggest that both minerals are concentrated in coarser sediment fractions, likely hosted within lithic particles (Fig. 5B, 5D, 6B, 6C). The enrichment of chlorite in the inner estuarine sand dominated catchment has previously been documented (Griffiths et al., 2018; Griffiths et al., 2019b), and chlorite within sand sized and lithic grains is commonly associated with the estuary head (Worden et al., 2020). Moreover, the influence of sub depositional environments on clay mineral distribution in the estuary surface and near surface sediments has also been well established (Griffiths et al., 2018; Griffiths et al., 2019b).

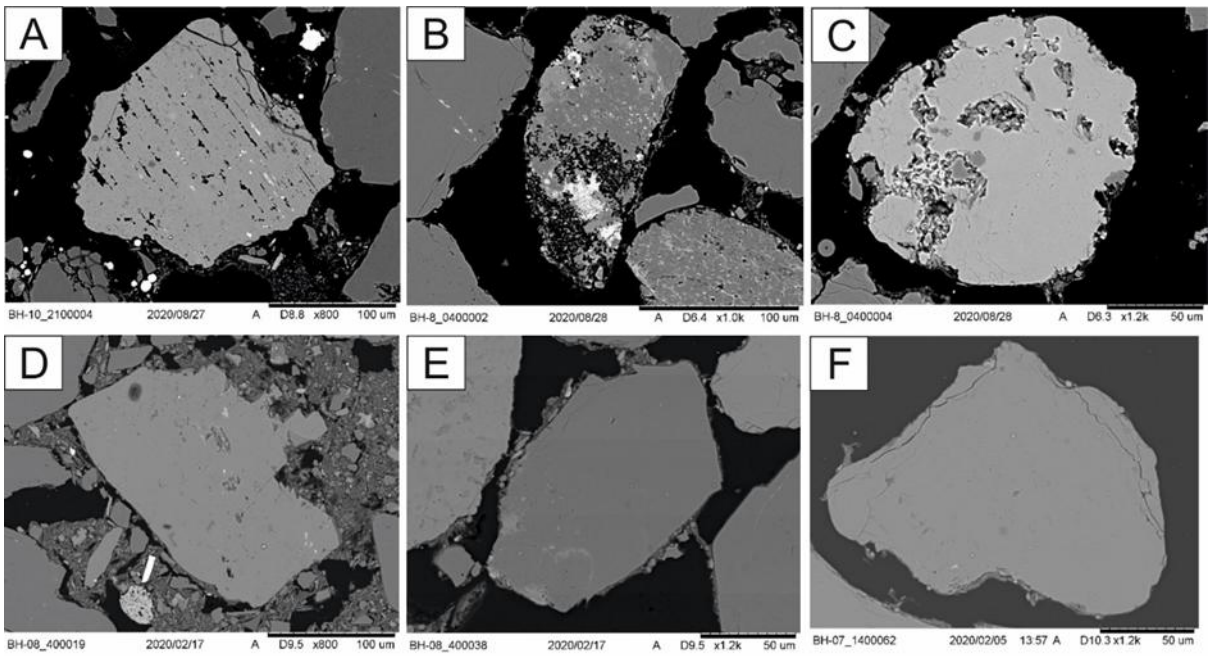

Figure 6. Scanning-electron-microscopy (SEM) images of (A) Muscovite alteration. (B) Plagioclase alteration. (C) Chlorite-biotite lithic grain. (D) clay-coated sand grains with coverage > 40%. (E) clay-coated sand grains with coverage < 40%. (F) clay-coated sand grains with coverage < 10%. Chlorite may occur as clay forming grain coat or as lithic grain in coarser sediment. The mineral alteration is dominantly observed in the coarser sediment and mostly associated with micas or feldspar lithic grains. In the salt marsh and mud flat sediment, clay occur as either pore filling or grain coating, with over 40% coat coverage. In the mixed flat and sand flat sediment, clay is mostly present as grain coat with reported coat coverage of less than 40%. The tidal inlet, foreshore and ebb-tidal-delta have a reported coat coverage of less than 10%.

Controls on clay distribution

Clay-mineral distribution in the studied Holocene sediment varies with sub-depositional environments due to interplay between several observed factors. These factors include provenance, weathering regime, grain-size and mineral morphology, flocculation due to water chemistry, in-situ alteration of detrital minerals, biological processes, and the transport mode of clay minerals (Edzwald and O'Mella, 1975; McIlroy et al., 2003; Worden and Morad, 2003; Brockamp and Zuther, 2004; Needham et al., 2004; Daneshvar and Worden, 2017). Previous research highlights provenance, hydrodynamics, sediment supply, and residence time as key factors governing clay-mineral distribution in the Holocene succession (Daneshvar and Worden, 2017; Griffiths et al., 2018; Griffiths et al., 2019a; Griffiths et al., 2019b). Clay minerals originate from weathering of Palaeozoic and Triassic bedrock, erosion of glacial till units, and landward sediment transport within the intertidal zone (Griffiths et al., 2018). Illite, the dominant clay mineral, has two main sources: Fe–Mg-rich illite from the Glacial Till Members (Griffiths et al., 2018), and Al-rich illite from feldspar alteration in the Eskdale Granite and Borrowdale Volcanic Group (Simpson, 1934; Young et al., 1986; Quirke et al., 2015). Kaolinite forms by silicate weathering within the estuary or hinterland, with additional input from Fishgarth Wood Till Member sediments (Griffiths et al., 2019b). Smectite develops during early stages of chemical weathering (Salem et al., 2000), and alteration of plagioclase to smectite is observed in coarser sediments (Fig. 6B). Chlorite is concentrated in high-energy, coarse-grained environments and commonly occurs within lithic grains; its distribution reflects fluvial delivery from chloritised Eskdale Granite (Griffiths et al., 2018; Griffiths et al., 2019b).

Both physicochemical processes (Grim and Johns, 1954; Powers, 1957; Nelson, 1960) and biological activity (McKinley et al., 2003; Needham et al., 2004; Needham et al., 2005; Needham et al., 2006; Worden et al., 2006) influence clay-mineral diagenesis. Earlier work has documented neoformation of kaolinite and illite from alteration of plagioclase and K-feldspar, respectively (Daneshvar and Worden, 2017), though other studies argue kaolinite derives mainly from intense feldspar alteration in the hinterland (Moseley, 1978; Young et al., 1986; Quirke et al., 2015). In the present study, plagioclase grains show rapid alteration to smectite (Fig. 6B). Alteration and dissolution of phyllosilicates, including meteoric-water–driven leaching at shallow depths (<20 m), is well documented (Ehrenberg and Nadeau, 1989; Scotchman et al., 1989; Bjørlykke, 1998; Barshep and Worden, 2021). Grain-size exerts a strong influence, with most alteration occurring in coarser, sand-dominated sub-environments (Fig. 6). Hydrodynamic processes play a major role in controlling estuarine sediment texture and clay-mineral distribution (Dalrymple et al., 1992; Gibbs, 1977). Previous studies have shown that clay-mineral patterns are strongly governed by hydrodynamics (Griffiths et al., 2018; Griffiths et al., 2019b), a conclusion reaffirmed by this study. Chlorite is most abundant in coarse, high-energy sub-depositional environments, where it commonly occurs within sand-grade lithic grains (Fig. 4A, 4F, 5A; Fig. 6C). In contrast, illite dominates fine-grained, low-energy settings such as mud flats and salt marshes, reflecting deposition under quiescent conditions along the inner-estuary margins and central basin (Fig. 4A, 4L, 5D). Kaolinite flocculates at low salinity and aggregates rapidly (Whitehouse et al., 1960; Edzwald & O'Mella, 1975), promoting early upstream deposition at the fluvial–marine interface; however, its abundance remains relatively uniform across the estuary because intense tidal mixing suppresses differential settling, consistent with earlier findings (Griffiths et al., 2018; Fig. 5B). Although overall smectite concentrations are low, it is relatively enriched in high-energy environments where it is linked to plagioclase alteration (Fig. 5C; Fig. 6B). Some studies have attributed low smectite abundance in coastal systems to tidal flushing and offshore export (Edzwald & O'Mella, 1975; McKinley et al., 2003; Worden & Burley, 2003). Mechanical-infiltration experiments (Matlack et al., 1989) suggest stratified clay distributions in sand bodies, with illite and smectite percolating downward while chlorite becomes trapped as coats. In contrast, the West Cumbria Holocene cores show only slight smectite increases with depth and no systematic vertical mineral changes (Fig. 4.6), matching prior observations from the Ravenglass and Gironde estuaries (Griffiths et al., 2018; Virolle et al., 2019). Previous work (Griffiths et al., 2018) has explained why the West Cumbria sediments do not follow the mechanical-infiltration model

Detrital clay grain coats

Clay-coat coverage, clay fraction, and clay-mineral distributions displayed a broadly similar patterns across the palaeo-sub-depositional environments (Fig. 4), indicating that the clay coats are largely detrital in origin (Griffiths et al., 2018). These coverage patterns in Holocene cores closely match those of surface and near-surface estuarine sediments (Fig. 4 and 6) (Wooldridge et al., 2017a; Wooldridge et al., 2017b; Griffiths et al., 2018), suggesting that primary depositional signatures are been preserved and the effect of post-depositional processes on clay distribution and clay coat coverage is negligible. Clay-fraction abundance and clay-coat coverage are therefore controlled by estuarine hydrodynamics, resulting in a predictable pattern of distributions across sub-depositional settings. Furthermore, high-energy outer-estuary zones such as the tidal inlet, foreshore, and ebb-tidal delta contain little to no clay coats due to low suspended load (Fig. 4D; 6F), whereas low-energy inner-estuary and central-basin settings show extensive coat development (Fig. 4D; 6D; 6E). Additionally, the similarity between Holocene and surface-sediment coat distributions further indicates negligible mechanical infiltration, tidal pumping, lateral porewater flow, or bioturbation during burial (Wooldridge et al., 2017b; Griffiths et al., 2018; Wooldridge et al., 2019a). An overlying clay-rich saltmarsh and mud-flat unit acts as an impermeable cap that inhibits downward clay transport and porewater movement (Fig. 4.3–4.6) (Griffiths et al., 2018b). Additionally, flocculation of clay and silt particles likely clogs pore spaces, limiting clay penetration into coarser

Dahiru Danjuma Muhammed, "Understanding the Controls on Clay Minerals Distribution in Modern Estuarine Sediments Through Integrated Geochemical and Petrographic Analysis," *International Research Journal of Advanced Engineering and Science*, Volume 11, Issue 1, pp. 145-156, 2026.

sediment (Buurman et al., 1998).

The observed relationship between clay fraction and clay-coat coverage (Fig. 4B; 4D) aligns with numerous studies on marginal-marine clay-coat distributions (Griffiths et al., 2018; Dowey et al., 2017; Virolle et al., 2020; Wooldridge et al., 2017b; Virolle et al., 2019). Clay-coat coverage in the sand-flat and tidal-bar sediments (Fig. 4D; 6E) lies within the optimum range reported to preserve porosity in deeply buried sandstones (Heald and Baker, 1977; Pittman et al., 1992; Bloch and Helmold, 1995; Bloch et al., 2002; Wooldridge et al., 2017b). Because ancient chlorite coats typically form through recrystallisation of precursor detrital coats (Bloch et al., 1997; Aagaard et al., 2000; Billault et al., 2003), the West Cumbria Holocene clay coats—resembling inner-layer detrital coats in deeply buried reservoirs (Wise et al., 2001; Ajdukiewicz and Larese, 2012; Worden et al., 2020)—serve as valuable analogues for predicting chlorite-coat development and porosity preservation in subsurface sandstone reservoirs.

IV. CONCLUSION

This study applies a geochemistry-based classification scheme, developed using the supervised RPART routine in R, to automatically discriminate palaeo–sub-depositional environments within Holocene core sediments from the West Cumbria, NW England.

Petrographic analysis show that the dominant mineral assemblage of these sediments comprises quartz, K-feldspar, plagioclase, muscovite, biotite, illite, chlorite, kaolinite, and smectite. Plagioclase and K-feldspar distributions are independent of grain-size variation but differ between sub-depositional environments, whereas biotite and muscovite are most abundant in the finer-grained settings and vary substantially across environments.

Clay-mineral distributions also show strong spatial variability. Chlorite is most enriched in the sand-flat and tidal-inlet environments and consistently low in the mud flat, mixed flat, and salt-marsh settings; it commonly occurs as a grain-coat clay or within lithic grains in coarser sediments. Kaolinite reaches its highest abundance in the mixed-flat environment but remains relatively uniform across the north foreshore, ebb-tidal delta, tidal inlet, sand flat, mud flat, and salt marsh. Smectite is most abundant in the ebb-tidal delta, north foreshore, and tidal inlet, with low concentrations in the mud-flat and salt-marsh zones. Illite is highest in the salt-marsh and mud-flat settings and shows broadly uniform distribution elsewhere.

Clay-coat coverage increases with clay-fraction abundance. In the salt-marsh and mud-flat sediments, clay occurs as both pore-filling and grain-coating material, exceeding 40% coverage. In the mixed-flat and sand-flat environments, clay occurs predominantly as grain coats, reaching coverage values up to approximately 40%. The tidal inlet, foreshore, and ebb-tidal delta display much lower coat coverage, reaching up to about 7%.

Sand-flat and tidal-bar sediments in the study area contain more than 10% detrital clay-coat coverage and include chlorite-bearing lithic grains have the potential to develop diagenetic chlorite coats capable of preserving anomalously high porosity by limiting quartz cementation during deep burial.

Overall, the spatial patterns of mineralogy and clay-mineral distributions within the core samples are primarily controlled by grain size and estuarine hydrodynamics. Early diagenetic processes specially feldspar alteration in coarser sediments have further modified clay-mineral distributions.

REFERENCES

[1]. Aagaard, P., Jahren, J.S., Harstad, A.O., Nilsen, O., Ramm, M., 2000. Formation of grain-coating chlorite in sandstones. Laboratory synthesized vs. natural occurrences. Clay Minerals 35, 261-269.
[2]. Ajdukiewicz, J.M., Lander, R.H., 2010. Sandstone reservoir quality prediction: The state of the art. American Association of Petroleum Geologists Bulletin 94, 1083-1091.
[3]. Ajdukiewicz, J.M., Larese, R.E., 2012. How clay grain coats inhibit quartz cement and preserve porosity in deeply buried sandstones: Observations and experiments. American Association of Petroleum Geologists Bulletin 96, 2091-2119.
[4]. Allen, G.P., Posamentier, H.W., 1994. Transgressive facies and sequence architecture in mixed tide-and wave-dominated incised valleys: example from the Gironde Estuary, France.
[5]. Aller, R.C., Aller, J.Y., 1998. The effect of biogenic irrigation intensity and solute exchange on diagenetic reaction rates in marine sediments. Journal of Marine Research 56, 905-936.
[6]. Aller, R.C., Michalopoulos, P., 1999. Invited lecture: Tropical, mobile mud belts as global diagenetic reactors. Geochemistry of the Earth's Surface, 289-292 pp.
[7]. Barnes, R., Ambrose, K., Holliday, D., Jones, N., 1994. Lithostratigraphical subdivision of the Triassic Sherwood sandstone group in west Cumbria. Proceedings of the Yorkshire Geological Society 50, 51-60.
[8]. Barshep, D.V., Worden, R.H., 2021. Reservoir Quality of Upper Jurassic Corallian Sandstones, Weald Basin, UK. Geosciences 11, 446.
[9]. Beaufort, D., Rigault, C., Billon, S., Billault, V., Inoue, A., Inoue, S., Patrier, P., 2015. Chlorite and chloritization processes through mixed-layer mineral series in low-temperature geological systems – a review. Clay Minerals 50, 497-523.
[10]. Berner, E.K., Berner, R.A., 2012. Global environment: water, air and geochemical cycles. Second edition. Princeton University Press, Princeton, 444 pp.
[11]. Berner, R.A., 1980. Early diagenesis: a theoretical approach. Princeton University Press.
[12]. Billault, V., Beaufort, D., Baronnet, A., Lacharpagne, J.C., 2003. A nanopetrographic and textural study of grain-coating chlorites in sandstone reservoirs. Clay Minerals 38, 315-328.
[13]. Bjørlykke, K., 1998. Clay mineral diagenesis in sedimentary basins - a key to the prediction of rock properties. Examples from the North Sea Basin. Clay Minerals 33, 15-34.
[14]. Bloch, S., Gjelberg, J., Dreyer, T., 1997. Preservation of anomalously high reservoir quality in deeply-buried, chlorite-coated, shallow marine sandstones (abs.): AAPG Annual Convention, Program with Abstracts, v. 6, p. A12.
[15]. Bloch, S., Helmold, K.P., 1995. Approaches to predicting reservoir quality in sandstones. American Association of Petroleum Geologists Bulletin 79, 97-115.
[16]. Bloch, S., Lander, R.H., Bonnell, L., 2002. Anomalously high porosity and permeability in deeply buried sandstone reservoirs: Origin and predictability. American Association of Petroleum Geologists Bulletin 86, 301-328.
[17]. Bokuniewicz, H., 1995. Chapter 3 Sedimentary Systems of Coastal-Plain Estuaries. In: G.M.E. Perillo (Ed.), Developments in Sedimentology. Elsevier, pp. 49-67.
[18]. Bousher, A., 1999. West Cumbria Estuary: Basic characteristics and evaluation of restoration options.
[19]. Boyle, E., Collier, R., Dengler, A.T., Edmond, J.M., Ng, A.C., Stallard, R.F., 1974. Chemical mass balance in estuaries. Geochimica et Cosmochimica Acta 38, 1719-1728.
[20]. Boyle, E.A., Edmond, J.M., Sholkovitz, E.R., 1977. Mechanism of iron removal in estuaries. Geochimica et Cosmochimica Acta 41, 1313-1324.

Dahiru Danjuma Muhammed, "Understanding the Controls on Clay Minerals Distribution in Modern Estuarine Sediments Through Integrated Geochemical and Petrographic Analysis," *International Research Journal of Advanced Engineering and Science*, Volume 11, Issue 1, pp. 145-156, 2026.

[21]. Brockamp, O., Zuther, M., 2004. Changes in clay mineral content of tidal flat sediments resulting from dike construction along the Lower Saxony coast of the North Sea, Germany. Sedimentology 51, 591-600.
[22]. Buurman, P., Jongmans, A.G., PiPujol, M.D., 1998. Clay illuviation and mechanical clay infiltration — Is there a difference? Quaternary International 51-52, 66-69.
[23]. Carr, A.P., Blackley, M.W.L., 1986. Implications of sedimentological and hydrological processes on the distribution of radionuclides: the example of a salt marsh near West Cumbria, Cumbria. Estuarine, Coastal and Shelf Science 22, 529-543.
[24]. Chamley, H., 1989. Clay Sedimentology. Springer-Verlag.
[25]. Dalrymple, R.W., Zaitlin, B.A., Boyd, R., 1992. Estuarine facies models - conceptual models and stratigraphic implications. Journal of Sedimentary Petrology 62, 1130-1146.
[26]. Daneshvar, E., 2015. Dissolved iron behavior in the West Cumbria Estuary waters, an implication on the early diagenesis. Universal Journal of Geoscience 3, 1-12.
[27]. Daneshvar, E., Worden, R.H., 2017. Feldspar alteration and Fe minerals: origin, distribution and implications for sandstone reservoir quality in estuarine sediments. Geological Society, London, Special Publications 435, SP435. 417.
[28]. Dowey, P.J., Hodgson, D.M., Worden, R.H., 2012. Pre-requisites, processes, and prediction of chlorite grain coatings in petroleum reservoirs: A review of subsurface examples. Marine and Petroleum Geology 32, 63-75.
[29]. Dowey, P.J., Worden, R.H., Utley, J., Hodgson, D.M., 2017. Sedimentary controls on modern sand grain coat formation. Sedimentary Geology 353, 46-63.
[30]. Drever, J.I., Zobrist, J., 1992. Chemical weathering of silicate rocks as a function of elevation in the southern Swiss Alps. Geochimica et Cosmochimica Acta 56, 3209-3216.
[31]. Eberl, D.D., Farmer, V.C., Barrer, R.M., 1984. Clay Mineral Formation and Transformation in Rocks and Soils [and Discussion]. Philosophical Transactions of the Royal Society of London A: Mathematical, Physical and Engineering Sciences 311, 241-257.
[32]. Edzwald, J.K., O'Mella, C.R., 1975. Clay distributions in recent estuarine sediments. Clays and Clay Minerals 23, 39-44.
[33]. Ehrenberg, S.N., 1993. Preservation of anomalously high-porosity in deeply buried sandstones by grain coating chlorite - examples from the Norwegian continental shelf. American Association of Petroleum Geologists Bulletin 77, 1260-1286.
[34]. Ehrenberg, S.N., Nadeau, P.H., 1989. Formation of diagenetic illite in sandstones of the Garn Formation, Haltenbanken area, mid-Norwegian continental shelf. Clay Minerals 24, 233-253.
[35]. Entwisle, D., Hobbs, P., Jones, L., Gunn, D., Raines, M., 2005. The relationships between effective porosity, uniaxial compressive strength and sonic velocity of intact Borrowdale Volcanic Group core samples from Sellafield. Geotechnical & Geological Engineering 23, 793-809.
[36]. Fan, D.J., Neuser, R.D., Sun, X.G., Yang, Z.S., Guo, Z.G., Zhai, S.K., 2008. Authigenic iron oxide formation in the estuarine mixing zone of the Yangtze River. Geo-Marine Letters 28, 7-14.
[37]. Feininger, T., 2013. An Introduction to the Rock-Forming Minerals (third edition). The Canadian Mineralogist 51, 663-664.
[38]. Fralick, P.W., Kronberg, B.I., 1997. Geochemical discrimination of clastic sedimentary rock sources. Sedimentary Geology 113, 111-124.
[39]. Gibbs, R.J., 1977. Transport phases of transition metals in the Amazon and Yukon Rivers. Geological Society of America Bulletin 88, 829-843.
[40]. Griffin, G.M., Ingram, R.L., 1955. Clay minerals of the Neuse River Estuary [North Carolina]. Journal of Sedimentary Research 25, 194-200.
[41]. Griffiths, J., Worden, R.H., Wooldridge, L.J., Utley, J.E., Duller, R.A., 2018. Detrital clay coats, clay minerals, and pyrite: a modern shallow-core analogue for ancient and deeply buried estuarine sandstones. Journal of Sedimentary Research 88, 1205-1237.
[42]. Griffiths, J., Worden, R.H., Wooldridge, L.J., Utley, J.E.P., Duller, R.A., 2019a. Compositional variation in modern estuarine sands: predicting major controls on sandstone reservoir quality. AAPG Bulletin 103, 797-833.
[43]. Griffiths, J., Worden, R.H., Wooldridge, L.J., Utley, J.E.P., Duller, R.A., Edge, R.L., 2019b. Estuarine clay mineral distribution: Modern analogue for ancient sandstone reservoir quality prediction. Sedimentology 66, 2011-2047.
[44]. Grim, R.E., Johns, W.D., 1954. Clay mineral investigations of sediments in the northern Gulf of Mexico. Clays and Clay Minerals 2nd National Conference Pergamon, New York, 81-103.
[45]. Haile, B.G., Hellevang, H., Aagaard, P., Jahren, J., 2015. Experimental nucleation and growth of smectite and chlorite coatings on clean feldspar and quartz grain surfaces. Marine and Petroleum Geology 68, 664-674.
[46]. Heald, M.T., Baker, G.F., 1977. Diagenesis of the Mt. Simon and Rose Run sandstones in western West Virginia and southern Ohio. Journal of Sedimentary Research 47, 66-77.
[47]. Huang, W.-L., 1993. Stability and kinetics of kaolinite to boehmite conversion under hydrothermal conditions. Chemical Geology 105, 197-214.
[48]. Kelly, M., Emptage, M., Mudge, S., Bradshaw, K., Hamilton-Taylor, J., 1991. The relationship between sediment and plutonium budgets in a small macrotidal estuary - Esk Estuary, Cumbria, UK. Journal of Environmental Radioactivity 13, 55-74.
[49]. Lander, R.H., Larese, R.E., Bonnell, L.M., 2008. Toward more accurate quartz cement models: The importance of euhedral versus noneuhedral growth rates. American Association of Petroleum Geologists Bulletin 92, 1537-1563.
[50]. Lloyd, J.M., Zong, Y., Fish, P., Innes, J.B., 2013. Holocene and Late-glacial relative sea-level change in north-west England: implications for glacial isostatic adjustment models. Journal of Quaternary Science 28, 59-70.
[51]. Matlack, K.S., Houseknecht, D.W., Applin, K.R., 1989. Emplacement of clay into sand by infiltration. Journal of Sedimentary Petrology 59, 77-87.
[52]. McGhee, C.A., Muhammed, D.D., Simon, N., Acikalin, S., Utley, J.E.P., Griffiths, J., Wooldridge, L.M., Verhagen, I.T.E., van der Land, C., Worden, R.H., 2021. Stratigraphy and sedimentary evolution of a modern macro-tidal incised valley– an analogue for reservoir facies and architecture. Sedimentology.
[53]. McIlroy, D., Worden, R.H., Needham, S.J., 2003. Faeces, clay minerals and reservoir potential. Journal of the Geological Society 160, 489-493.
[54]. McKinley, J.M., Worden, R.H., Ruffell, A.H., 2003. Smectite in sandstones: A review of the controls on occurrence and behaviour during diagenesis. In: Clay mineral cements in sandstones (eds. Worden, R.H. and Morad, S.) International Association of Sedimentologists Special Publications 34, 109-128.
[55]. Merritt, J.W., Auton, C.A., 2000. An outline of the lithostratigraphy and depositional history of Quaternary deposits in the Sellafield district, west Cumbria. Proceedings of the Yorkshire Geological Society 53, 129-154.
[56]. Michalopoulos, P., Aller, R.C., 1995. Rapid clay mineral transformation in Amazon Delta sediments - reverse weathering and oceanic element cycles. Science 270, 614-617.
[57]. Michalopoulos, P., Aller, R.C., 2004. Early diagenesis of biogenic silica in the Amazon delta: Alteration, authigenic clay formation, and storage. Geochimica et Cosmochimica Acta 68, 1061-1085.
[58]. Michalopoulos, P., Aller, R.C., Reeder, R.J., 2000. Conversion of diatoms to clays during early diagenesis in tropical, continental shelf muds. Geology 28, 1095-1098.
[59]. Millward, D., 2004. A stratigraphical framework for the upper Ordovician and Lower Devonian volcanic and intrusive rocks in the English Lake District and adjacent areas. 0852724004, British Geological Survey Research Report.
[60]. Milodowski, A., Gillespie, M., Naden, J., Fortey, N., Shepherd, T., Pearce, J., Metcalfe, R., 1998. The petrology and paragenesis of fracture mineralization in the Sellafield area, west Cumbria. Proceedings of the Yorkshire Geological Society 52, 215-241.
[61]. Moseley, F., 1978. The geology of the Lake District. Yorkshire Geological Society.
[62]. Muhammed, D.D., Simon, N., Utley, J.E.P., Verhagen, I.T.E., Duller, R.A., Griffiths, J., Wooldridge, L.J., Worden, R.H., 2022, in press. Geochemistry of Sub-Depositional Environments in Estuarine Sediments: Development of an Approach to Predict Palaeo-Environments from Holocene Cores. Geosciences.
[63]. Muhammed, D.D., Worden, R.H., Simon, N., Utley, J.E.P., Verhagen, I.T.E., Duller, R.A., Griffiths, J., Wooldridge, L.M., in press. Prediction of palaeo-sub-depositional environments in estua-rine surface and Holocene sands using bulk elemental compositions. Geosciences.
[64]. Needham, S.J., Worden, R.H., Cuadros, J., 2006. Sediment ingestion by worms and the production of bio-clays: a study of macrobiologically

enhanced weathering and early diagenetic processes. Sedimentology 53, 567-579.
[65]. Needham, S.J., Worden, R.H., McIlroy, D., 2004. Animal-sediment interactions: the effect of ingestion and excretion by worms on mineralogy. Biogeosciences 1, 113-121.
[66]. Needham, S.J., Worden, R.H., McIlroy, D., 2005. Experimental production of clay rims by macrobiotic sediment ingestion and excretion processes. Journal of Sedimentary Research 75, 1028-1037.
[67]. Nelson, B.W., Clay mineralogy of the bottom sediments, Rappahannock River, Virginia. In, Clays and Clay Minerals: Proceedings of the Seventh National Conference on Clays and Clay Minerals Washington, DC, USA, 20–23 October 1958; Elsevier: Amsterdam. 1960, Washington, DC, USA. Elsevier, pp. 135-148.
[68]. Pittman, E.D., Larese, R.E., Heald, M.T., 1992. Clay coats: occurrence and relevance to preservation of porosity in sandstones. In: Origin, diagenesis and petrophysics of clay minerals in sandstones (eds. Houseknecht, D.W. and Pittman, E.D.) SEPM Special Publication 47, 241-255.
[69]. Powers, M.C., 1957. Adjustment of land derived clays to the marine environment. Journal of Sedimentary Research 27.
[70]. Quirke, J., Henderson, C., Pattrick, R., Rosso, K., Dent, A., Sharples, J., Pearce, C., 2015. Characterizing mineralogy and redox reactivity in potential host rocks for a UK geological disposal facility. Mineralogical Magazine 79, 1353-1367.
[71]. R Core Team, 2016. R: A language and environment for statistical computing. R Foundation for Statistical Computing, Vienna, Austria.
[72]. Rateev, M.A., Sadchikova, T.A., Shabrova, V.P., 2008. Clay minerals in recent sediments of the World Ocean and their relation to types of lithogenesis. Lithology and Mineral Resources 43, 125-135.
[73]. Rundle, C., 1979. Ordovician intrusions in the English Lake District. Journal of the Geological Society 136, 29-38.
[74]. Saïag, J., Brigaud, B., Portier, E., Desaubliaux, G., Bucherie, A., Miska, S., Pagel, M., 2016. Sedimentological control on the diagenesis and reservoir quality of tidal sandstones of the Upper Cape Hay Formation (Permian, Bonaparte Basin, Australia). Marine and Petroleum Geology 77, 597-624.
[75]. Salem, A.M., Morad, S., Mato, L.F., Al-Aasm, I.S., 2000. Diagenesis and reservoir-quality evolution of fluvial sandstones during progressive burial and uplift: Evidence from the Upper Jurassic Boipeba Member, Reconcavo basin, northeastern Brazil. American Association of Petroleum Geologists Bulletin 84, 1015-1040.
[76]. Scotchman, I.C., Johnes, L.H., Miller, R.S., 1989. Clay diagenesis and oil migration in Brent Group sandstones of NW Hutton Field, UK North Sea. Clay Minerals 24, 339-374.
[77]. Simon, N., Worden, R.H., Muhammed, D.D., Utley, J.E.P., Verhagen, I.T.E., Griffiths, J., Wooldridge, L.J., 2021. Sediment textural characteristics of the West Cumbria Estuary; Development of a method to predict palaeo sub-depositional environments from estuary core samples. Sedimentary Geology 418, 105906.
[78]. Simpson, B., 1934. The petrology of the Eskdale (Cumberland) granite. Proceedings of the Geologists' Association 45, 17-34.
[79]. Sionneau, T., Bout-Roumazeilles, V., Biscaye, P.E., Van Vliet-Lanoe, B., Bory, A., 2008. Clay mineral distributions in and around the Mississippi River watershed and Northern Gulf of Mexico: sources and transport patterns. Quaternary Science Reviews 27, 1740-1751.
[80]. Soper, N., 1987. The Ordovician batholith of the English Lake District: Correspondence and Notes. Geological Magazine 124, 481-482.
[81]. Storvoll, V., Bjørlykke, K., Karlsen, D., Saigal, G., 2002. Porosity preservation in reservoir sandstones due to grain-coating illite: a study of the Jurassic Garn Formation from the Kristin and Lavrans fields, offshore Mid-Norway. Marine and Petroleum Geology 19, 767-781.
[82]. Strong, G.E., Milodowski, A.E., Pearce, J.M., Kemp, S.J., Prior, S.V., Morton, A.C., The petrology and diagenesis of Permo-Triassic rocks of the Sellafield area, Cumbria. In, Proceedings of the Yorkshire Geological and Polytechnic Society. 1994, Geological Society of London, pp. 77-89.
[83]. Therneau, T., Atkinson, E., 2019. An introduction to recursive partitioning using rpart routines: The Comprehensive R Archive Network. CRAN.
[84]. Thiry, M., 2000. Palaeoclimatic interpretation of clay minerals in marine deposits: an outlook from the continental origin. Earth-Science Reviews 49, 201-221.
[85]. Tucker, M.E., 2001. Sedimentary petrology: an introduction to the origin of sedimentary rocks. John Wiley & Sons.
[86]. Velde, B., Church, T., 1999. Rapid clay transformations in Delaware salt marshes. Applied Geochemistry 14, 559-568.
[87]. Virolle, M., Brigaud, B., Bourillot, R., Féniès, H., Portier, E., Duteil, T., Nouet, J., Patrier, P., Beaufort, D., 2019. Detrital clay grain coats in estuarine clastic deposits: origin and spatial distribution within a modern sedimentary system, the Gironde Estuary (south-west France). Sedimentology 66, 859-894.
[88]. Virolle, M., Féniès, H., Brigaud, B., Bourillot, R., Portier, E., Patrier, P., Beaufort, D., Jalon-Rojas, I., Derriennic, H., Miska, S., 2020. Facies associations, detrital clay grain coats and mineralogical characterization of the Gironde estuary tidal bars: A modern analogue for deeply buried estuarine sandstone reservoirs. Marine and Petroleum Geology 114, 104225.
[89]. Whitehouse, U.G., Jeffrey, L.M., Debbrecht, J.D., 1960. Differential settling tendencies of clay minerals in saline waters. Clays and Clay Minerals 7, 1-79.
[90]. Wilson, M.D., 1992. Inherited grain-rimming clays in sandstones from eolian and shelf environments: their origin and control on reservoir properties. In: Origin, diagenesis and petrophysics of clay minerals in sandstones (eds. Houseknecht, D.W. and Pittman, E.D.) SEPM Special Publication 47, 209-225.
[91]. Windom, H.L., 1976. Lithogenous material in marine sediments. Chemical Oceanography 5, 103-135.
[92]. Wise, S., Smellie, J., Aghib, F., Jarrard, R., Krissek, L., 2001. Authigenic smectite clay coats in CRP-3 drillcore, Victoria Land Basin, Antarctica, as a possible indicator of fluid flow: a progress report. Terra Antartica 8, 281-298.
[93]. Wooldridge, L.J., Worden, R.H., Griffiths, J., Thompson, A., Chung, P., 2017a. Biofilm origin of clay-coated sand grains. Geology 45, 875-878.
[94]. Wooldridge, L.J., Worden, R.H., Griffiths, J., Utley, J.E.P., 2017b. Clay-coated sand grains in petroleum reservoirs: Understanding their distribution via a modern analogue. Journal of Sedimentary Research 87, 338-352.
[95]. Wooldridge, L.J., Worden, R.H., Griffiths, J., Utley, J.E.P., 2019a. Clay-coat diversity in marginal marine sediments. Sedimentology 66, 1118-1138.
[96]. Wooldridge, L.J., Worden, R.H., Griffiths, J., Utley, J.E.P., 2019b. How to quantify clay-coat grain coverage in modern and ancient sediments. Journal of Sedimentary Research 89, 135-146.
[97]. Wooldridge, L.J., Worden, R.H., Griffiths, J., Utley, J.E.P., Thompson, A., 2018. The origin of clay-coated sand grains and sediment heterogeneity in tidal flats. Sedimentary Geology 373, 191-209.
[98]. Worden, R.H., Burley, S.D., 2003. Sandstone Diagenesis: The Evolution of Sand to Stone, Sandstone Diagenesis, pp. 1-44.
[99]. Worden, R.H., Griffiths, J., Wooldridge, L.J., Utley, J.E.P., Lawan, A.Y., Muhammed, D.D., Simon, N., Armitage, P.J., 2020. Chlorite in sandstones. Earth-Science Reviews 204, 103105.
[100]. Worden, R.H., Morad, S., 2003. Clay minerals in sandstones: Controls on formation, distribution and evolution. In: Clay mineral cements in sandstones (eds. Worden, R.H. and Morad, S.) International Association of Sedimentologists Special Publications 34, 3-41.
[101]. Worden, R.H., Needham, S.J., Cuadros, J., 2006. The worm gut; a natural clay mineral factory and a possible cause of diagenetic grain coats in sandstones. Journal of Geochemical Exploration 89, 428-431.
[102]. Young, B., Fortey, N.J., Nancarrow, P.H.A., 1986. An occurrence of tungsten mineralisation in the Eskdale Intrusion, West Cumbria. Proceedings of the Yorkshire Geological Society 46, 15-21.
[103]. Zhang, J., Wen Huang, W., Chong Shi, M., 1990. Huanghe (Yellow River) and its estuary: Sediment origin, transport and deposition. Journal of Hydrology 120, 203-223.